Intensity Characteristics of the Noctuid Acoustic Receptor

WILLIAM B. ADAMS

From the Laboratory of Sensory Communication, Syracuse University, Syracuse, New York 13210. Dr. Adams's present address is the School of Electrical Engineering, Purdue University, Lafayette, Indiana 47907.

ABSTRACT Spiking activity of the more sensitive acoustic receptor is described as a function of stimulus intensity. The form of the intensity characteristic depends strongly on stimulus duration. For very brief stimuli, the integral of stimulus power over stimulus duration determines the effectiveness. No response saturation is observed. With longer stimuli (50 msec), a steady firing rate is elicited. The response extends from the spontaneous rate of 20–40 spikes/sec to a saturated firing rate of nearly 700 spikes/sec. The characteristic is monotonic over more than 50 db in stimulus intensity. With very long stimuli (10 sec), the characteristics are nonmonotonic. Firing rates late in the stimulus decrease in response to an increase in stimulus intensity. The nonmonotonic characteristics are attributed to intensity-related changes in response adaptation.

INTRODUCTION

The acoustic receptor of the noctuid moth is admirably suited for the study of receptor mechanisms. Each ear contains only two acoustic receptor cells and the transduction activity appears to be contained within these nerve cells. There are no synapses in the periphery, no efferent controls, and no interactions between the cells. A third receptor cell, the B cell, is found on the Bügel, an exoskeletal projection within the ear. The axons from the acoustic receptor cells and the B cell are contained in a sheath and form the auditory nerve; the spike responses of all three axons can be recorded from the nerve with gross electrodes.

It has been found that the two acoustic receptor cells, although similar in most response parameters, differ in their sensitivity by 20 db or more (Roeder and Treat, 1957; Suga, 1961). The nerve fiber associated with the more sensitive receptor has been designated as the A-1 fiber, and the other as the A-2 fiber. The B fiber responds to distortions of the epithelial sheath surrounding the Bügel, but not to acoustic stimulation (Treat and Roeder, 1959).

The purpose of this paper is to describe in detail the change in the response

of the A-1 receptor as a function of stimulus intensity. Spiking activity is used as a measure of the neural response magnitude. The results indicate that the duration of the stimulus plays an important role. The use of very short stimuli allows an investigation of the temporal integration of stimulus power. No response saturation is observed with these stimuli. With moderate-duration stimuli, the firings become regular and the intensity characteristics are monotonic over a wide range of stimulus intensities. Precise measures of the firing rates are obtained and compared with several proposed descriptions of sensory intensity characteristics. Very long–duration stimuli reveal the effects of adaptation and subsequent nonmonotonic intensity characteristics. The simplicity of this receptor suggests that many of the intensity-dependent phenomena find their origin in the transuction process. Thus, the results obtained should provide some insights into the performance of the transducer.

The noctuid acoustic receptor has also been the subject of several investigations in behavioral physiology. Roeder and his colleagues have shown that its primary function is the detection of bat cries with subsequent triggering of evasive behavior (Roeder and Treat, 1961; Roder, 1962, 1966, 1967; Roeder and Payne, 1966). Detailed descriptions of the receptor anatomy may also be found in their articles (Roeder and Treat, 1957; Treat, 1959; Treat and Roeder, 1959) and in older works by Richards (1932) and Eggers (1919). The fine structure of the receptor organ has been described recently by Ghiradella (1971), providing a structural basis for future studies of the mechanism of transduction.

METHODS AND MATERIALS

Live Materials Approximately 150 moths served in the experiments. Preliminary investigations were carried out on various noctuid species caught at light on summer evenings. Subsequently, specimens of *Prodenia eridania*, Cramer were obtained as adults from the Niagara Chemical Div., FMC Corp., Middleport, N. Y. The data in this report stem from these laboratory-reared moths.

Anatomy The acoustic receptor organs are placed bilaterally at the thoracoabdominal juncture. A thin, semitransparent tympanic membrane (*T*) is partially exposed to impinging sound waves (Fig. 1, top). It is supported on three sides by exoskeleton, on the fourth by the conjunctivum (*Cj*) or accessory tympanic membrane. These two membranes form the external wall of the tympanic cavity, a local enlargement of the tracheal system. A countertympanic cavity is found in the abdomen, separated from the tympanic cavity by the countertympanic membrane (*CTM*). The two acoustic receptor cells are contained within a scoloparium (*S*) that is suspended in the tympanic cavity between the tympanic membrane and the Bügel (*B*, Fig. 1, bottom).

Methods The moth was anesthetized temporarily with carbon dioxide. A small well was melted in a paraffin-filled cup and the animal was plunged head down into the molten wax to the level of the mesothoracic legs. When the wax had hardened, the wings were severed close to the body wall, and the metathoracic

legs were cut or broken off at the coxaltrochanter articulation. The abdomen was removed to expose the countertympanic membranes (*CTM*).

A dissection pin inserted through the soft tissues of the thoracic cavity and into the wax prevented gross movements of the animal, and served as a common (ground) electrode. (In some experiments, the ground connection consisted of a silver–silver chloride electrode. The electrode reduced the recorded DC potential, but did not otherwise affect the recording or life of the preparation.)

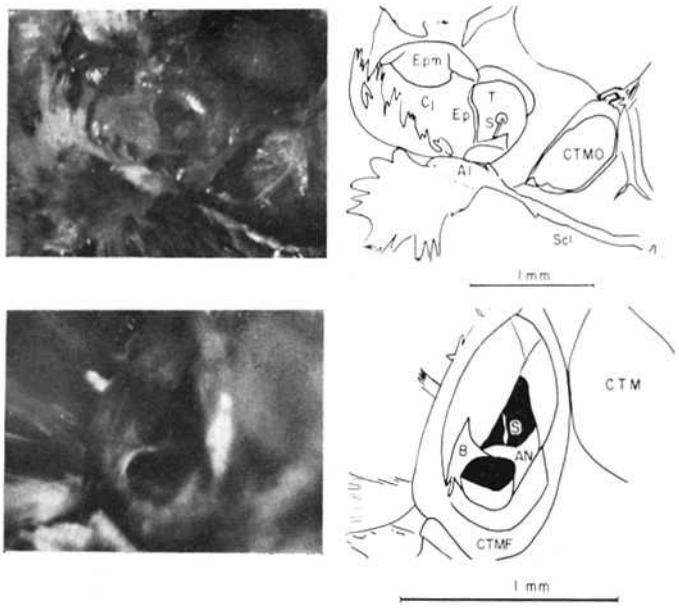

FIGURE 1. *Top*, caudal view of the acoustic receptor organ. The scutellum (*Scl*) marks the dorsal margin of the thorax. The legs, wings, abdomen, countertympanic membrane, and hood (an exoskeletal structure parallel and caudal to the tympanic membrane) have been removed. The scoloparium (*S*) can be seen through the transparent tympanic membrane. *Bottom*, the tympanic cavity as seen through the countertympanic membrane orifice. *Al*, alula; *AN*, auditory nerve; *B*, Bügel; *Cj*, conjunctivum; *CTM*, countertympanic membrane; *CTMF*, exoskeletal frame that supports edges of CTM; *CTMO*, orifice resulting from excision of CTM; *Ep*, epaulette; *Epm*, epimeron; *S*, scoloparium; *Scl*, scutellum; *T*, tympanic membrane. Top micrograph × 16.5; bottom micrograph × 29.

The scales on the alula (*Al*), at the edge of the conjunctivum (*Cj*), and on the scutellum (*Scl*) were removed with forceps. The countertympanic membranes were severed at their medial borders and lifted free. The auditory nerve could then be seen at the lateral edge of the orifice, running from the Bügel to the rostral wall of the tympanic cavity (Fig. 1, bottom). A recording pipette filled with buffered saline was positioned with its tip near the auditory nerve close to the Bügel (the pipettes and saline are described below). A small drop of saline expelled from the tip of the pipette facilitated electrical contact with the dry nerve sheath. The saline did not

touch the scoloparium. The audio monitor was turned on and the pipette advanced manually to attain electrical contact. The most obvious signs of contact consisted of a drop in the monitor noise level and the appearance of spike activity. Acoustic stimulation was then applied and, if necessary, the position of the pipette was adjusted to obtain good quality recordings from the auditory fiber.

The output of the recording electrode was led to a high impedance preamplifier (Picometric 180A, Instrumentation Laboratory Inc., Watertown, Mass.), amplified 1000 times (Type 122, Tektronix Inc., Beaverton, Ore.), and recorded on magnetic tape (Model 3907B, Hewlett-Packard Co., Palo Alto, Calif.). Synchronization signals and voice commentary were recorded simultaneously. The firing patterns were analyzed during the experiment in terms of poststimulus time (PST) response histograms with a Fabri-Tek computer (Type 1062 with SW-2C and SH-1 plug-ins, Fabri-Tek Instruments, Inc., Madison, Wis.). The same system served for analysis of recorded data.

Approximately one-third of the experiments were successful. Failures could be attributed to three causes: poor quality recordings; rapid deterioration of the preparation; or rapid movements of the animal, resulting in large recording artifacts. Successful preparations maintained stable responses for a minimum of 30 min–1 hr. Rarely, a preparation remained stable for up to 4 hr. Most experiments were designed to allow a full set of measurements for each animal within approximately ½ hr. A rapid decline of spontaneous activity and response sensitivity usually signalled deterioration of a previously stable preparation.

Recording Pipettes The recording pipettes closely resembled those used as suction electrodes. Micropipettes (about 1 μ diameter) were drawn from precleaned 1 mm KG-33 capillary tubing on an Eccles-type vertical puller (Type PE-2, Narishige, Labtron Scientific Corp., Farmingdale, N.Y.). The tips were broken, examined under a compound microscope, and retained only if the broken ends appeared reasonably square and between 12 and 18 μ in diameter. The broken ends were heat-polished on the electrode puller and reexamined to ascertain that all rough edges had been removed.

Just before use, saline was injected into a pipette. A length of flexible Tygon tubing (Tygon Plastic Tubing, Chamberlain Engineering Corp., Akron, Ohio) was slipped over the end of the pipette for expelling fluid from the pipette tip. A silver–silver chloride wire that passed through the tubing into the end of the pipette provided the electrical connection.

The saline that filled the pipettes was modified from Pringle (1938). The pH of the solution appeared to be a critical factor in obtaining stable preparations, and the saline was thus heavily buffered with phosphate at pH 7.0–7.1. Calcium was omitted from Pringle's formulation to prevent precipitation of $CaHPO_4$. Before each experiment, the solution was made up from stock solutions of 0.2 M NaH_2PO_4, 0.2 M Na_2HPO_4, and saline containing 0.308 M Na^+, 5.9 mM K^+, and 0.314 M Cl^-. The stock solutions were made up weekly, or more often when needed. The final concentrations of the electrode filling solution were: Na^+, 335 mM; K^+, 2.7 mM; Cl^-, 157 mM; phosphate (as $H_2PO_4^-$ and $HPO_4^=$), 100 mM.

Acoustic Source A small condenser microphone (Bruel and Kjaer, Cleveland, Ohio, type 4136; 0.25 inch diaphragm) served as the transmitter of acoustic stimuli.

In early preparations, the transmitter was operated in the nonpolarized, frequency-doubling mode. In later experiments, a DC polarization of 180 v was applied. The AC input at 0 db amounted to 70 v rms in the nonpolarized mode and to 15 v in the polarized mode. For stimulation, the transmitter was pointed toward the tympanic recess and positioned at a distance of about 5 mm. Because of the geometry of the system, i.e. neither truly closed cavity nor free field, and the limitation of the transmitter to low sound intensities, the sound pressure at the eardrum was estimated by comparing the results to the established threshold levels for similar noctuid moths (Roeder, 1966). For frequencies between 40 and 80 kHz, the sound pressure without attenuation was estimated at 70 db *re* 0.0002 dynes/cm^2, allowing ± 5 db for frequency response and calibration error.

RESULTS

Short-Duration Stimuli The response to short-duration stimuli was determined by means of acoustic stimuli with fast (<0.015 msec) rise and fall times. For stimuli that had durations comparable to the membrane time constant of about 1 msec (Adams, 1970), the response approximated an impulse response, and the time-course did not depend on the stimulus duration (Fig. 2 *a*, *b*, *c*). For longer stimuli, the duration of the response increased (Fig. 2 *d*). Thus, the total number of spikes elicited by each stimulus was determined by the amplitude of the impulse response and the amplitude and duration of the extended response.

To provide a consistent measure of the responses, the average number of spikes, including spontaneous activity, was measured during the first 5 msec following the onset of the response. For the very short stimuli, most of the stimulus-related spikes appeared only at the beginning of the analysis period, while they were spread throughout for longer stimuli. The results of these measurements are shown in Fig. 3. An interesting feature of the data is the similarity among curves, not only the curves corresponding to the impulse response, but also those corresponding to the extended response. In addition, no response saturation occurs, although the intensities are comparable to those that saturate the response with longer stimulus durations (Figs. 7, 11). This appears to indicate that saturation is not directly dependent on stimulus intensity, but rather on the response magnitude. Because of the short duration of these stimuli, the response is small and no saturation occurs.

The lateral separation of the curves in Fig. 3 indicates that the integral of stimulus power over the stimulus duration determined the effectiveness of the stimulus. For example, in order to elicit a response to 8 out of 10 stimuli, the power required for a stimulus duration of 0.2 msec was one-half (-3 db) that for 0.1 msec, and 10 times ($+10$ db) that for a stimulus duration of 2.0 msec. The relationship applies to both the impulse-like stimuli and the longer stimuli, even though the time-course of the generator potentials produced by them should be quite dissimilar. Apparently the response of the cell is con-

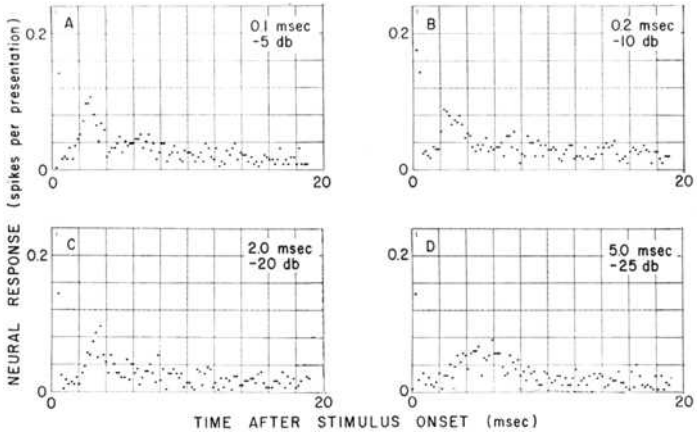

FIGURE 2. Time-course of spike response to brief stimuli. The stimulus durations in (*a*), (*b*), (*c*), and (*d*) are 0.1, 0.2, 2.0, and 5.0 msec, respectively. The intensities chosen elicit approximately equal responses during the first 5 msec (see Fig. 3). When the stimulus duration is comparable to the membrane time constant, or shorter, an approximate impulse response is elicited. When the duration is considerably longer than the time constant, the response duration is also lengthened (*d*).

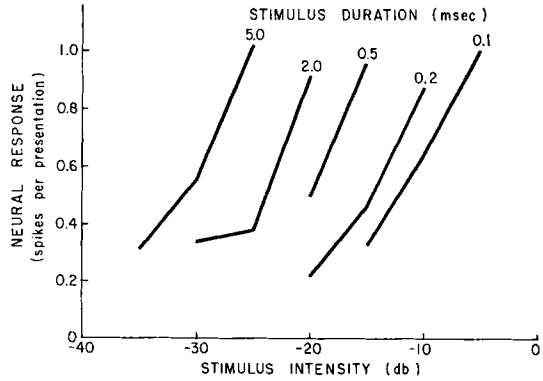

FIGURE 3. Time-intensity relationship for brief stimuli. The total number of spikes elicited during the first 5 msec of the response is shown as a function of stimulus duration and stimulus intensity. The results indicate that the magnitude of the neural response is determined by the time integral of stimulus power.

trolled by the time integral of the generator potential which is taken in such a way as to produce equivalence between the two situations.

Moderate-Duration Stimuli—the Standard Stimulus As the stimulus duration is increased, firing rate saturation is observed at high intensities. After some preliminary investigation of response parameters, a standard stimulus was chosen for further use. This stimulus consisted of a tone burst of 50 msec duration, plus rise and fall times of 2.5 msec each. The repetition rate was 1/sec. The following factors entered into the selection of the standard stimulus.

(*a*) The stimulus is long enough to obtain a measure of the response elicited during the second half of the stimulus. Thus, it is possible to exclude from the measure any effects arising from stimulus transients or a phasic response of the nerve cell. The effective firing rate, determined during the second half of the stimulus, provides a sensitive stable measure of excitation (see following results).

(*b*) The duration is short enough to avoid appreciable adaptation. During the stimulus, the firing rate is constant to within 10% (discussed more fully later). The smallest adaptation time constant amounted to 1.25 sec (next section), predicting a maximum adaptation decrement of 4%.

(*c*) A low duty cycle (5%) allows ample time for neural recovery between stimuli. Spontaneous activity, which is depressed immediately following a stimulus, recovers its normal rate before the next stimulus. Moreover, the average response elicited by each stimulus in a series of 50 remains constant throughout the series.

The typical response to the stimuli after recording, playback, and filtering is shown in Fig. 4. The rate of discharge of the large spikes that appear randomly throughout the records was not influenced by acoustic stimulation. These spikes are assigned therefore to the nonacoustic B fiber. Most of the remaining spikes in Fig. 4 are from the more sensitive A-1 acoustic fiber. In some instances, small spikes from the A-2 fiber can be seen although, for the most part, they are hidden in the base-line noise. In the few experiments where spikes were recorded from both acoustic fibers, the spikes from the A-1 fiber were always larger than those from the A-2 fiber, in agreement with results of other workers. In preparations where the acoustically driven spikes were uniform in size and apparently originated from a single fiber, the response threshold corresponded to that of the A-1 fiber.

The stimulus was on during the first half of the sweeps shown in Fig. 4. At the lowest intensity (-40 db), there seems to be little, if any, stimulus-related activity. As the intensity was increased, more and more spikes were elicited by each stimulus. At the higher intensities, the firing rate during stimulation became quite regular. In all experiments with high intensity stimuli, the size of the spikes appeared to increase at the higher firing rates (Fig. 4, -15 db), apparently as an artifact of the recording arrangement.

A more extensive sample of the firing patterns is shown in the dotgrams of Fig. 5. Each spike has been reduced to a dot, and each row corresponds to a separate stimulus sweep. Here, even at the lowest intensity, it can be seen that spikes appear slightly more often during the stimulus than after it. At the highest intensity, the spike trains are very regular, and even superimposable over the first half of the stimulus.

As a first step toward a quantitative response measure, PST histograms were generated of the times of occurrence of the A-1 spikes (Fig. 6). The responses to 50 stimuli were used in each case. The alternating maxima and minima

during the first half of the high intensity stimuli are the result of the spike-train overlap mentioned above. During the second half of the stimuli, synchrony between spike trains is lost and the histograms are smoother. From this point until the end of the stimulus, the response is constant.

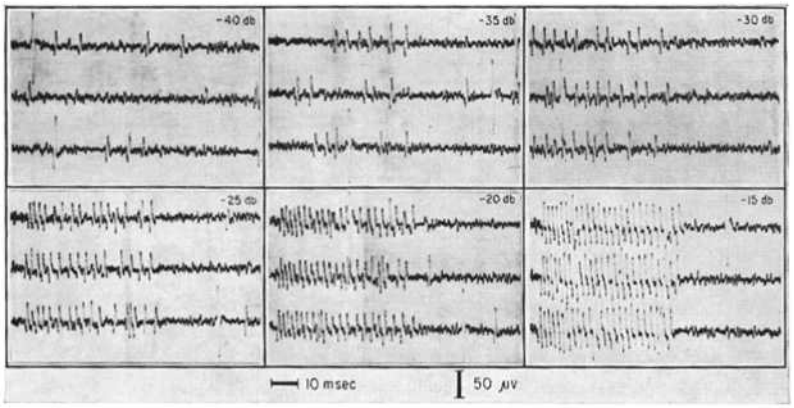

FIGURE 4. Tympanic nerve response. After recording, playback, and filtering, the spikes from the A-1 fiber are biphasic, approximately 50 μv in amplitude. The large spikes that appear randomly are from the B fiber. Very small spikes from the A-2 fiber can be seen occasionally, but for the most part they are hidden in the base-line noise. The stimulus was on during the first half of each sweep with intensities as indicated (repetition rate: 1/sec). The time and voltage calibration is constant throughout.

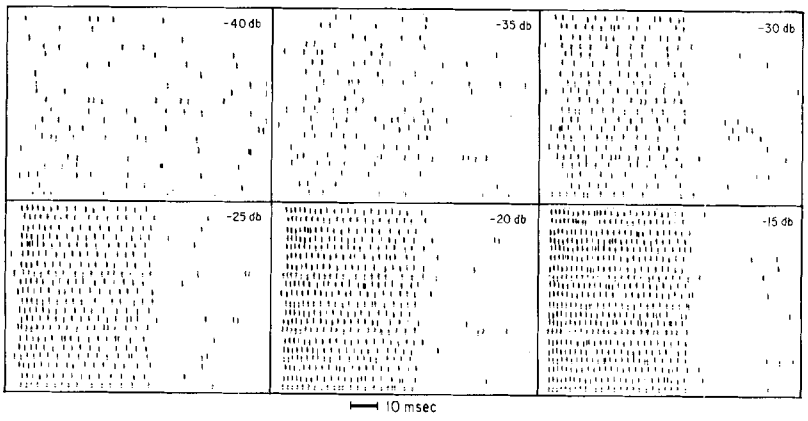

FIGURE 5. Dotgrams of spike responses. The recordings of Fig. 3 were passed through a voltage discriminator to reduce each spike to a dot (both A-1 and B fiber spikes are included). The trace is moved slightly down after each sweep.

The interval of constant response provides a convenient analysis period for calculation of an effective neural firing rate. The calculation is accomplished by dividing the total number of spikes elicited during the 50 analysis periods by the total analysis time (50 × 25 msec). Since the quantity being measured and averaged is the number of spikes, rather than instantaneous frequency,

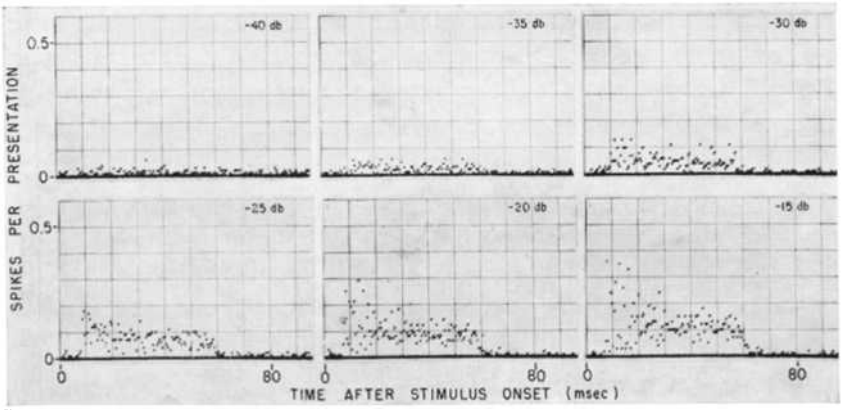

FIGURE 6. Poststimulus time histograms generated from responses of the A-1 fiber. Each point represents the average number of spikes during a 0.5 msec analysis interval. The data are from the same experiment as shown in Figs. 4 and 5. The responses to 50 stimuli were used in generating each histogram.

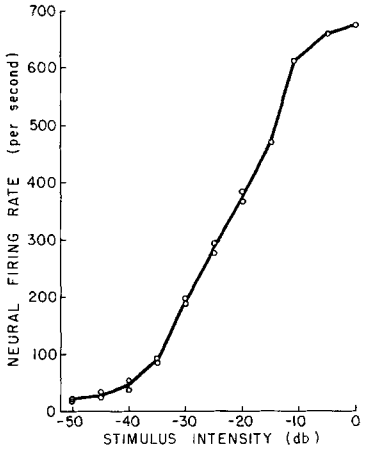

FIGURE 7

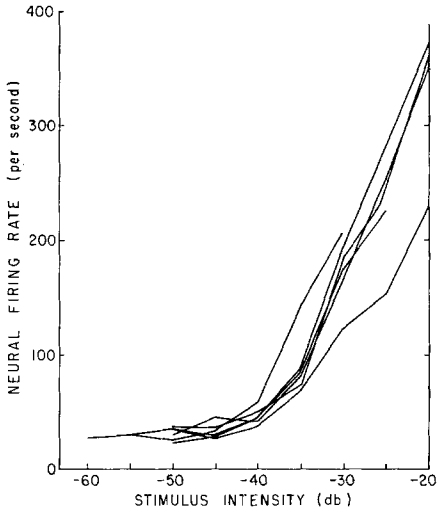

FIGURE 8

FIGURE 7. Neural firing rate as a function of intensity. The data were obtained from a single preparation. The stimulus was 50 msec in duration, delivered once per second. The effective firing rate was calculated from the responses elicited during the last 25 msec of each stimulus. The responses to 50 stimuli were used for each measurement. For intensities between −50 and −20 db, the firing rate was determined once at the beginning and again later in the experiment. The responses to the four highest intensities (−15 through 0 db) were measured at the end of the experiment.

FIGURE 8. Intensity characteristics from six preparations, determined as in Fig. 7. In each instance, the stimulus frequency was that which required the lowest voltage input to the transducer for excitation of the receptor. The frequencies ranged from 52.47 to 81.93 kHz. In most experiments, the use of high intensities was avoided.

"effective firing rate" seems preferable to "average firing rate." In any event, the measure provides a useful and consistent indication of the magnitude of the neural response.

The intensity characteristic of Fig. 7 was obtained by plotting the effective firing rate as a function of stimulus intensity. The response to each intensity was determined twice in alternating ascending and descending series. The agreement between measurements gives an indication of the stability of the response measure. In most experiments, very intense stimuli were avoided. The responses to the four highest intensities in Fig. 7 were determined at the end of the experiment and are included here for completeness.

The intensity characteristic is not only stable during an experiment, it is remarkably consistent from animal to animal. To illustrate this point, Fig. 8 shows the characteristics of six preparations. Because of the similarity of intensity functions from animal to animal, the sensitivity of the receptor to a particular stimulus, e.g. of some specified frequency, is determined completely by the response to an arbitrarily chosen suprathreshold intensity. Once the response is known, the intensity that would elicit a "criterion response" can be determined by reference to a standard intensity function. A response rate of 50 spikes/sec was chosen as the criterion response (the rate of spontaneous activity lies between 20 and 40 spikes/sec; Adams, 1970). The intensity functions of Fig. 8 were shifted horizontally so as to coincide at 50 spikes/sec, and averaged arithmetically at 5-db intervals. The "standard intensity characteristic" thus obtained is shown in Fig. 9. The abscissa gives the stimulus intensity relative to

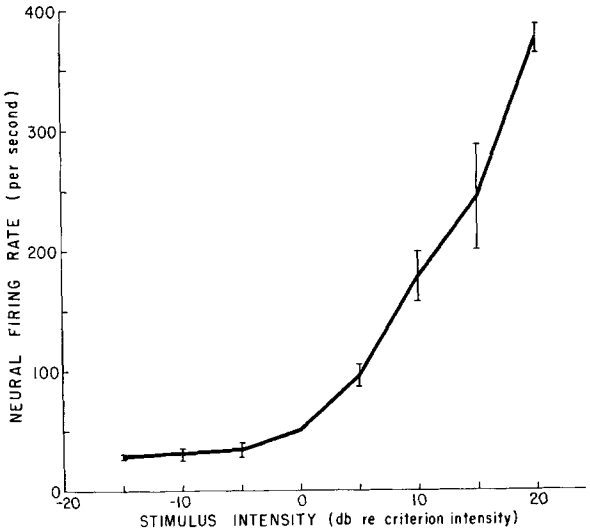

FIGURE 9. Standard intensity characteristic. The results of the six experiments shown in Fig. 8 were used to compute the means. The abscissa gives the stimulus intensity referred to the intensity that is required to elicit the criterion response of 50 spikes/sec. Vertical bars: ± 1 sample SD.

that which would produce a criterion response. The ordinate is the neural firing rate in spikes per second, as before. The vertical bars indicate ±1 SD of the sample in terms of the effective firing rate. The standard deviation in terms of intensity is never greater than 2.5 db. Thus, for firing rates between 50 and 200/sec—a fairly easy range to find experimentally—the extrapolation to the criterion intensity is in error by usually no more than 2.5 db.

Long-Duration Stimuli Qualitatively different intensity characteristics were obtained with long-duration stimuli. The plots of firing rate in Fig. 10 show results of one experiment that is typical of several performed with 10-sec stimuli. 5 min were allowed for recovery between stimuli. Intensities of −30, −20, −10, and 0 db were delivered in ascending order, and of −5, −15, −25, and −35 db in descending order (not shown in this figure). In all the histo-

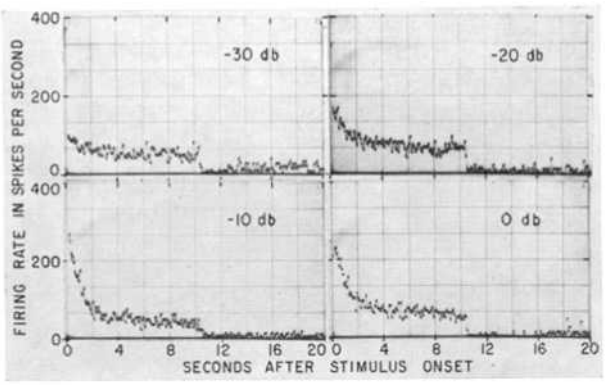

FIGURE 10. Response to long-duration stimuli. 10-sec stimuli were used, with intensities as indicated. The neural firing rate is averaged over 100 msec for each point. Pronounced adaptation occurs during the first 2 sec of the response, followed by more moderate adaptation for the remainder of the response.

grams there is an initial stage of exponential adaptation lasting for 2 sec, followed by a period of slower adaptation. At −10 db, the firing rate decreases by more than 75% during the first 1 sec with an additional decrease of only 40% during the next 8 sec.

The initial adaptation produces some rather unusual results. When the firing rate is measured at different times during the response, the intensity functions of Fig. 11 are obtained. Shortly after the stimulus onset (0.25 and 1 sec), the firing rates increase monotonically with intensity until saturation. When measured at 2 sec from onset, however, a dip appears in the intensity function at −10 db. At 10 sec after the stimulus onset, the firing rate actually decreases by 50% in response to a 10 db increment in stimulus intensity. It may be of interest, from a functional point of view, to note that nonmonotonic intensity functions are also observed in mammalian auditory nerve fibers in

response to certain long-duration stimuli (Kiang et al., 1969). However, in light of the greater complexity of the mammalian system, different causes may well underlie the effect in the two systems.

The shape of the intensity functions in the moth's receptor can be attributed almost completely to the form of the initial adaptation. Although the duration

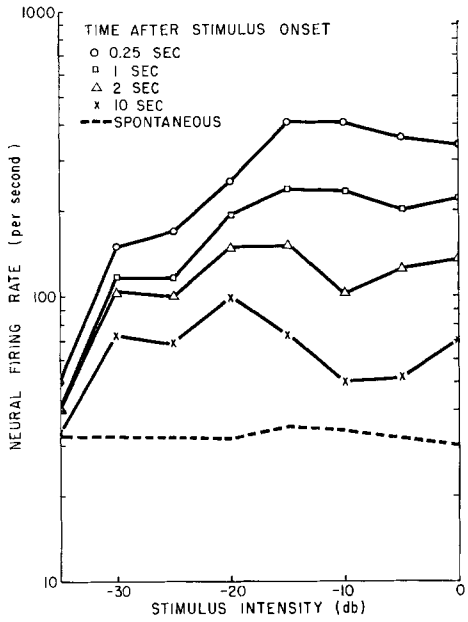

FIGURE 11

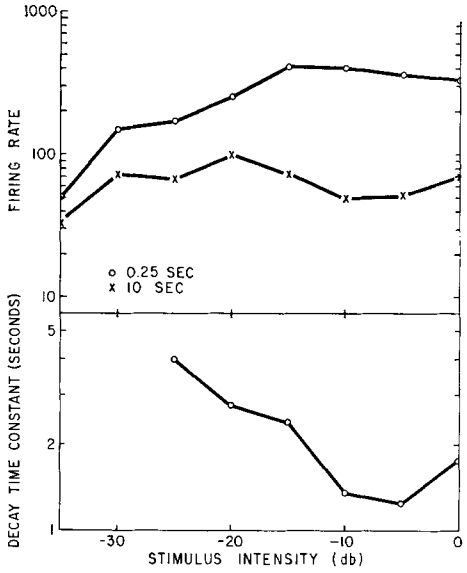

FIGURE 12

FIGURE 11. Intensity characteristics for response to long-duration stimuli. 10-sec stimuli were used. The firing rates were measured from the response histograms, including those in Fig. 10 at various delays from the stimulus onset. The rate of spontaneous activity (dashed line) was measured immediately before each stimulus presentation and was constant throughout the series. Data are from one experiment.

FIGURE 12. Adaptation time constant. The time constant of the initial adaptation (lower graph) was measured from the response histograms. Two of the intensity characteristics from the previous figure are repeated (upper graph) to illustrate the association between rapid adaptation (small time constants) and the nonmonotonic portions of the intensity characteristic.

is nearly constant at about 2 sec, the rate of adaptation changes markedly with stimulus intensity. In Fig. 12, the rate of adaptation is plotted in terms of the decay time constant along with the firing rates that were measured at 0.25 and 10 sec from the stimulus onset. The lowest intensity at which a reliable measure of the adaptation time constant could be obtained was -25 db. At this intensity, the time constant was large, just over 4 sec, corresponding to an initial adaptation of less than 40%. As the stimulus intensity increased, the time

constant decreased sharply, reaching a minimum of approximately 1.3 sec at −5 db. The data of Fig. 12 show that the smallest time constants, and hence the most rapid adaptation, are found at exactly those intensities where the dip in the intensity function occurs. Thus, although a nearly steady-state firing rate is reached after the initial 2 sec of adaptation, the firing rate attained is so strongly dependent on the adaptation characteristics as to make it an inadequate descriptor of receptor sensitivity.

DISCUSSION

When short-duration stimuli are employed, the stimulus intensity can be adjusted for a constant neural response. The results reveal that the response is determined by the time integral of stimulus power. Thus, under these conditions, the effectiveness of the mechanical stimulus depends on the square of the displacement amplitude, rather than on the linear amplitude. Nevertheless, at some point between the physical stimulus and the neural firing rate, the large dynamic range of the physical stimuli must be reduced to the smaller range of neural firing rates. If the dependence on stimulus power applies under all stimulus-response conditions, the stimulus compression must be doubled. In Fig. 7, for example, the dynamic range encompasses 2.5 decades in stimulus displacement and 5 decades in stimulus power while the neural firing rate covers only 1.5 decades.

A second approach for evaluating the effectiveness of a stimulus is to examine the change in neural firing rate as a function of stimulus intensity rather than the intensity required for a constant response. For this purpose, the data obtained with moderate-duration stimuli are useful. A question often asked in sensory physiology is whether neural intensity characteristics can be described by logarithmic or power functions. To test these possibilities, the standard intensity characteristic has been plotted on both log-linear and log-log coordinates. In the log-linear plot (Fig. 13, left side), a straight line has been fitted to the portion of the curve between +5 and +30 db greater than the criterion intensity. The fit is quite good (correlation coefficient 0.993), so that this portion of the curve appears logarithmic. In the log-log plot (right side), the spontaneous activity has been subtracted from the firing rate and a straight line fitted to the portion of the curve between −15 and +10 db. Again the fit is good (correlation coefficient 0.996), so that this portion appears to be a power function. The comparison shows that either a logarithmic or a power function provides a good approximation to limited segments of the intensity characteristic. However, neither provides so accurate a description as to exclude other functional forms.

Efforts to fit physiological intensity characteristics with logarithmic or power functions are due mainly to the influence of psychophysics. A reasonable

fit to the data is usually obtained for a limited range of stimulus intensities, but discrepancies nearly always arise at one or both extremes of the dynamic range. A number of mathematical formulations have been suggested to de-

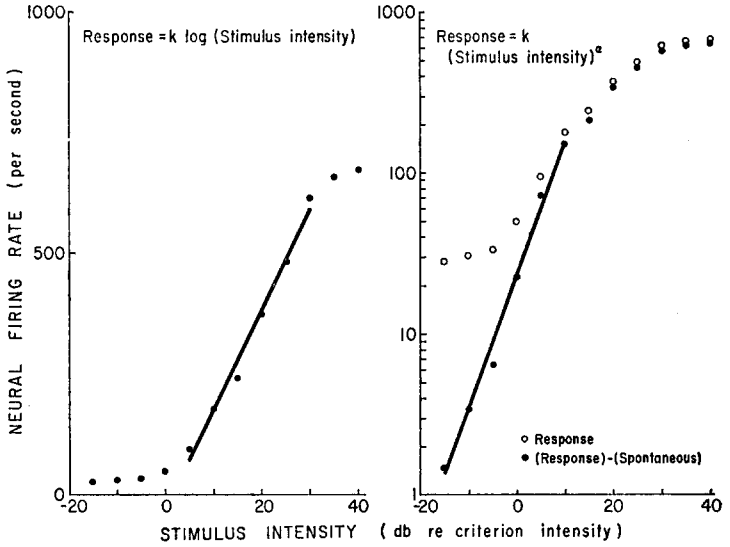

FIGURE 13. Logarithmic and power function approximations to the intensity characteristic. *Left*, the neural response is plotted on a linear scale and the stimulus power on a logarithmic (decibel) scale. A straight line described by response = k log (stimulus power) is fitted to the data between 5 and 30 db. *Right*, the neural response (open circles) and the net driven response (total response minus spontaneous activity, closed circles) are plotted on a logarithmic scale; the stimulus power is also on a logarithmic (decibel) scale. A straight line describing the driven response as a power function of stimulus intensity (i.e. response = k [stimulus power]$^{\alpha}$) has been fitted to the data between -15 and $+10$ db.

sribe the entire intensit y characteristic. The relationship

$$\text{response} = \frac{kbx}{1 + bx} \qquad (1)$$

was first introduced by Loewenstein (1961) to describe the amplitude of generator potentials obtained from isolated, denuded pacinian corpuscles. The original derivation was intended to apply to generator potentials elicited by stimuli of limited spatial extent, so that x ($0 \leq x \leq 1$) represented the stimulated fraction of the membrane and, hence,the proportion of activated receptor sites. The constant of proportionality, k, depended on the resting potential and the site of the external recording electrode, while the scaling factor, b, provided a measure of the effectiveness of a particular stimulus. However, it

can be shown that the parameters can be interpreted more generally without affecting the form of the relationship. If x ($0 \leq x \leq \infty$) represents the conductance of the transduction sites, then the constants b and k can be expressed in terms of the resting potential, the transducer equilibrium potential, and the conductance of the nontransducing portion of the membrane.

On the assumption that the firing rate is related linearly to the amplitude of the generator potential (Fuortes, 1958; Terzuolo and Washizu, 1962), and if the relationship between conductance and stimulus intensity is known, then equation 1 can be used to predict the firing rate as a function of intensity. Alternatively, if the variation of conductance with intensity is not known, it can be deduced from measured firing rates with the aid of equation 1. Taking the latter approach, the constant of proportionality is given by the maximum firing rate, about 680/sec. The assumption of a residual transducer conductance in the unstimulated state provides for spontaneous activity. Using the data of Fig. 9, the best fit over the entire range of intensities was obtained when the conductance followed a power function of displacement:

$$x \propto (\text{displacement})^{1.7} + (\text{residual conductance}). \qquad (2)$$

Other functional forms, such as logarithmic or exponential, provided poor approximations. The intensity characteristic described by equations 1 and 2 is shown in Fig. 14 (left side), superimposed on the average data points. The agreement is good a both ends of the dynamic range, but poor in the center. However, the significance of the agreement is unclear. Finding that the transducer conductance varies as a power function of displacement is not particularly satisfying as an indication of the mechanisms involved. Of course, further measurement—in particular, direct recording of the generator potential—may show the power function to be only an approximation of the true state of affairs.

The Loewenstein formula really is applicable only to generator potential amplitudes and an additional transformation may be necessary for an accurate prediction of the neural firing rate. In order to deal directly with the firing rate, Zwislocki (1969) has suggested

$$\frac{\text{total response}}{\text{spontaneous}} = \frac{1}{k}\left[1 - e^{-k\left(\frac{S}{N}+1\right)^{1/2}}\right] \qquad (2)$$

as a semiempirical description of intensity characteristics. In this equation, S is the stimulus power, N an internal noise, and k a constant defined functionally by the ratio of maximal to spontaneous firing rate. One advantage of this description is that N is the only free parameter and serves merely as a scaling factor without affecting the shape of the curve. The fit to this equation is shown in the right side of Fig. 14, with good agreement over the entire

dynamic range. In fact, equation 3 has provided accurate descriptions for the intensity characteristics of spontaneously active neurons of several sensory modalities (Zwislocki et al., 1969), with the implication that all sensory receptors share some common properties.

One interesting facet of this description is the dependence on the stimulus power, S. This dependence is in accord with the results of the studies with short-duration stimuli, where the response was determined by the time integral of stimulus power. Nevertheless, the present data do not allow a distinc-

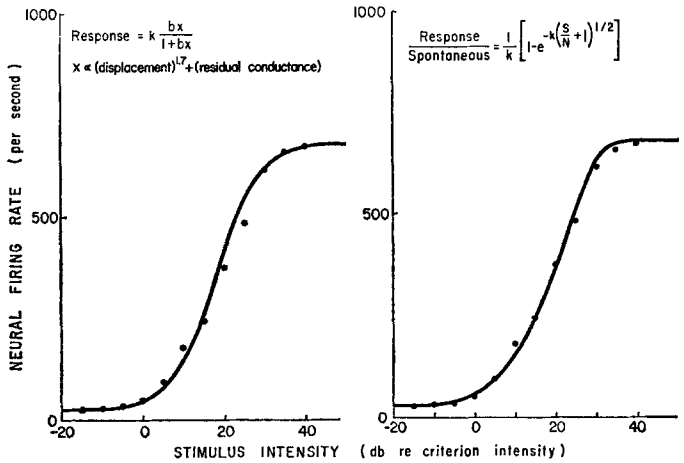

FIGURE 14. Complete approximations to the intensity characteristic. *Left*, a curve described by response $= k\,bx/(1 + bx)$ (Loewenstein, 1961) is fitted to the data. The transducer conductance, x, follows a power function of stimulus displacement. *Right*, a curve described by

$$\frac{\text{total response}}{\text{spontaneous}} = \frac{1}{k}\left[1 - e^{-k\left(\frac{S}{N}+1\right)^{1/2}}\right]$$

(Zwislocki, 1969) is fitted to the data. The term k is defined as the ratio of spontaneous to maximal firing rates, S is the stimulus power, and N an internal noise, chosen for the best fit to the data.

tion to be made between stimulus power and displacement amplitude squared. If it is found that the receptor is excited by constant displacement of the transduction region, i.e. stimulus power equal to zero, then S must be interpreted as displacement squared. Conversely, if movement is required, then the interpretation of S as stimulus power is accurate. Work is now underway to resolve this question.

The number of possible mechanisms that may contribute to long-term adaptation is reduced by the simplicity of the noctuid receptor organ. No synapses intervene between the transduction and spike generating sites, and no connections have been observed between the receptor cells (Ghiradella,

1971). Apparently, no efferent controls are present (Treat, 1959). In some mechanoreceptors, e.g. the encapsulated pacinian corpuscle (Loewenstein, 1965), adaptation effects have been traced to the mechanical system surrounding the receptor cell. Although it is not clear how this explanation would apply to time-varying deformations, there appears to be no conclusive way to rule out such effects. The remaining possible causes of adaptation result from changes in ionic permeabilities or concentrations at either the transduction or spike generation site. Decreases in generator potential amplitudes (Grundfest, 1965) and increases in spike generation thresholds (Nakajima, 1964) during long stimuli appear to be common occurrences in receptors. One clue is that the nonmonotonic intensity functions occur only after some 300 spikes have been elicited during the preceding 2 sec. This observation suggests that the ionic milieu, and thereby the excitability, is altered by the sustained high-level activity of the neuron. Since the effect is apparent only at high intensities, it is possible that the activity of the less-sensitive A-2 cell also contributes to the disturbance of the ionic environment. Intracellular recordings are now being undertaken to try to separate the adaptation effects that are due to transduction activity from those that are due to the spike generating process.

My thanks go to Doctors Robert B. Barlow, Jr. and Jozef J. Zwislocki for their assistance and counsel during the course of these studies and in the preparation of the manuscript. Live specimens of *Prodenia eridania* Cramer were provided throughout these studies by Mr. Dominic Albanese and Dr. Kenneth Ensing of the Niagara Chemical Div., FMC Corp.

This paper is based on a dissertation submitted to the faculty of Syracuse University in partial fulfillment of the requirements for the degree of Doctor of Philosophy.

This work was supported by Grant No. NS-03950 from the U. S. Department of Health, Education, and Welfare, National Institute of Neurological Diseases and Stroke. Manuscript preparation was supported by Grant No. 5-S04 RR 06013 from the Division of Research Resources, National Institutes of Health.

Received for publication 7 May 1971.

BIBLIOGRAPHY

ADAMS, W. B. 1970. Receptor characteristics in the tympanic organ of the noctuid moth. Special Report No. 8. Laboratory of Sensory Communication, Syracuse University.

Eggers, F. 1919. Das thoracale bitympanal Organ einer Gruppe der Lepidoptera Heterocera. *Zool. Jahrb. Abt. Anat. Ontog. Tiere.* **41**:273.

FUORTES, M. G. F. 1958. Electric activity of cells in the eye of *Limulus*. *Amer. J. Ophthalmol.* **46**:210.

GHIRADELLA, H. 1971. Fine structure of the noctuid moth ear. I. The transducer area and connections to the tympanic membrane in *Feltia subgothica* Haworth. *J. Morphol.* **134**:21.

GRUNDFEST, H. 1965. Electrophysiology and pharmacology of different components of bioelectric transducers. *Cold Spring Harbor Symp. Quant. Biol.* **30**:1.

KIANG, N. Y-S., T. BAER, E. M. MARR, and D. DERMOT. 1969. Discharge rates of single auditory-nerve fibers as functions of tone level. *J. Acoust. Soc. Amer.* **46**:106(A).

LOEWENSTEIN, W. R. 1961. Excitation and inactivation in a receptor membrane. *Ann. N. Y. Acad. Sci.* **94**:510.

LOEWENSTEIN, W. R. 1965. Facets of a transducer process. *Cold Spring Harbor Symp. Quant. Biol.* **30**:29.

NAKAJIMA, S. 1964. Adaptation in stretch receptor neurons of crayfish. *Science (Washington).* **146:**1168.

PRINGLE, J. W. S. 1938. Proprioception in insects. I. A new type of mechanical receptor from the palps of the cockroach. *J. Exp. Biol.* **15:**101.

RICHARDS, A. G. 1932. Comparative skeletal morphology of the noctuid tympanum. *Entomol. Amer.* **13:**1.

ROEDER, K. D. 1962. The behavior of free flying moths in the presence of artificial ultrasonic pulses. *Anim. Behav.* **10:**300.

ROEDER, K. D. 1966. Acoustic sensitivity of the noctuid tympanic organ and its range for the cries of bats. *J. Insect Physiol.* **12:**843.

ROEDER, K. D. 1967. Turning tendency of moths exposed to ultrasound while in stationary flight. *J. Insect Physiol.* **13:**873.

ROEDER, K. D., and R. S. PAYNE. 1966. Acoustic orientation of a moth in flight by means of two sense cells. *Symp. Soc. Exp. Biol.* **20:**251.

ROEDER, K. D., and A. E. TREAT. 1957. Ultrasonic reception by the tympanic organ of noctuid moths. *J. Exp. Zool.* **134:**127.

ROEDER, K. D., and A. E. TREAT. 1961. The detection and evasion of bats by moths. *Amer. Sci.* **49:**135.

SUGA, N. 1961. Functional organization of two tympanic neurons in noctuid moths. *Jap. J. Physiol.* **11:**666.

TERZUOLO, C. H., and Y. WASHIZU. 1962. Relation between stimulus strength, generator potential and impulse frequency in stretch receptor of Crustacea. *J. Neurophysiol.* **25:**56.

TREAT, A. E. 1959. The metathoracic musculature of *Crymodes devastator* (Brace) (Noctuidae) with special reference to the tympanic organ. *Smithson. Misc. Collect.* **137:**365.

TREAT, A. E., and K. D. ROEDER. 1959. A nervous element of unknown function in the tympanic organs of moths. *J. Insect Physiol.* **3:**262.

ZWISLOCKI, J. J. 1969. A generalized intensity characteristic of sensory receptors. Semiannual Research Report, Laboratory of Sensory Communication, Syracuse University. **10:**7.

ZWISLOCKI, J. J., W. B. ADAMS, R. B. BARLOW, and E. J. KLETSKY. 1969. Intensity characteristics of sensory receptors. *Abstr. Int. Biophys. Congr. 3rd.* 262.